



You have downloaded a document from
RE-BUŚ
repository of the University of Silesia in Katowice

Title: Application of seismic parameters for estimation of destress blasting effectiveness

Author: Łukasz Wojtecki, Petr Konicek, Maciej J. Mendecki, Waław M. Zuberek

Citation style: Wojtecki Łukasz, Konicek Petr, Mendecki Maciej J., Zuberek Waław M. (2017). Application of seismic parameters for estimation of destress blasting effectiveness. "Procedia Engineering" (Vol. 191 (2017), s. 750-760), doi 10.1016/j.proeng.2017.05.241



Uznanie autorstwa - Użycie niekomercyjne - Bez utworów zależnych Polska - Licencja ta zezwala na rozpowszechnianie, przedstawianie i wykonywanie utworu jedynie w celach niekomercyjnych oraz pod warunkiem zachowania go w oryginalnej postaci (nie tworzenia utworów zależnych).



UNIwersYTET ŚLĄSKI
W KATOWICACH



Biblioteka
Uniwersytetu Śląskiego



Ministerstwo Nauki
i Szkolnictwa Wyższego



Symposium of the International Society for Rock Mechanics

Application of Seismic Parameters for Estimation of Destress Blasting Effectiveness

Łukasz Wojtecki^a, Petr Konicek^b, Maciej J. Mendecki^{c,d,*}, Waclaw M. Zuberek^c

^aPolish Mining Group, Powstancow 30, 40-039 Katowice, Poland

^bInstitute of Geonic of the CAS, Studentska 1768, 708 00 Ostrava-Poruba, Czech Republic

^cUniversity of Silesia in Katowice, Faculty of Earth Sciences, Bedzinska 60, Sosnowiec, Poland

^dCentre for Polar Studies KNOW (Leading National Research Centre), University of Silesia in Katowice, Bedzinska 60, Sosnowiec, Poland

Abstract

Coal seams in the Upper Silesian Coal Basin are currently extracted under more and more disadvantageous geological and mining conditions. Mining depth, geological dislocations and mining remnants are factors which affect the rockburst hazard during underground mining to the greatest extent. This hazard can be minimized by employment of active rockburst prevention, where long-hole destress blasts in roof rocks (torpedo blasts) have an important role. The main goal of these blastings is to either destress local stress concentrations in rock mass and to fracture the thick layers of strong roof rocks to prevent or minimize the impact of high energy tremors on the excavations. Sometimes, these blastings are performed to make the roof rocks caving behind the longwall face easier. The efficiency of blasting is typically evaluated from the seismic effect, which is calculated based on seismic monitoring data (seismic energy) and the weight of the charged explosive. This method, as used previously in the Czech Republic, was adopted in a selected Polish hard coal mine in the Upper Silesian Coal Basin. This method enables rapid and easy estimation of destress blasting effectiveness, adjusted to conditions occurring in the designed colliery. Destress blasts effectiveness may be evaluated via the seismic source parameters analysis as well, as was carried out in the selected colliery in the Polish part of the Upper Silesian Coal Basin. These parameters provide information, for example, on its size, state of stress and occurrence of slip mechanism in the source of provoked tremors. Long-hole destress blasting effectiveness in selected colliery has been evaluated using the seismic effect method and seismic source parameters analysis. The results were compared with each other and conditions were observed in situ.

© 2017 The Authors. Published by Elsevier Ltd. This is an open access article under the CC BY-NC-ND license (<http://creativecommons.org/licenses/by-nc-nd/4.0/>).

Peer-review under responsibility of the organizing committee of EUROCK 2017

Keywords: active rockburst prevention; long-hole destress blasting; seismic effect; seismic source parameters

* Corresponding author. Tel.: +48-693-477-700.
E-mail address: maciej.mendecki@us.edu.pl

1. Introduction

Rockburst is a dangerous phenomenon occurring during deep underground hard coal mining in the Upper Silesian Coal Basin (USCB). To minimize this hazard, special prevention techniques are applied. One of them are destress blasts in the rocks surrounding the coal seam, especially in roof rocks. The main purpose of such blasts is to reduce stress concentrations in these rocks, and to reach a new advantageous energy equilibrium state by the rock mass due to stress drop. Fracturing the thick layers of strong roof rocks to prevent or minimize the impact of high energy tremors on the excavations is important too. Sometimes blasts are performed to facilitate roof rocks caving and goaf formation. Hanging-up of strong roof rocks behind longwall face may be responsible for high-energy tremors occurrence in close distance from the longwall face, which is dangerous for the working crew.

The registered provoked tremor may be related only to detonation of a special weight of explosives or to additional processes in rock mass activated by blasting. Sometimes, the energy of provoked tremors is much higher than it would appear from the weight of used explosives. Such an effect suggests that blasting is more effective and some energy accumulated in the rock mass has been released.

Seismic energy of provoked tremors is at present the main parameter for estimation of blasting effectiveness in hard coal mines [1, 2, 3]. However, some attempts have been made to use the seismic source parameters for this purpose. Generally, these parameters characterize the focus of the tremor. Using these parameters, the size of tremor focus and state of stress in focus can be calculated. The type of process occurring in focus can be determined as well.

In this paper presents estimation of effectiveness of destress blasts performed within active rockburst prevention during longwall mining of coal seam no. 504 in one of the hard coal mines in the Polish part of the Upper Silesian Coal Basin. These blasts were performed in various configurations, including location and number of blastholes and applied weight of explosives. The said destress blasts were also performed under variable geological and mining conditions. Provoked tremors have been analyzed with the use of their seismic parameters.

2. Geological and mining conditions

Coal seam no. 504 in the area of the selected longwall is deposited at the depth from 865 to 910 m. The stress level at such a depth, according to the weight of local blanket rock, exceeds 20 MPa. The thickness of coal seam no. 504 varies from 3.2 m to 6.8 m. During presence of high-energy tremors, the floor heave couldn't be excluded.

The direct roof of coal seam no. 504 is composed of alternating layers of shale, sandy shale and sandstone, but sandy shales and sandstones dominate. These rocks manifest a tendency to hanging-up behind the longwall face. During fracturing of such tough rocks, a high-energy tremor might occur. Above the mentioned rocks, a layer of sandstones occurs, up to 60 m thick. The uniaxial comprehensive strength of these sandstones reaches maximum 80 MPa. Potentially, fracturing of this layer was able to generate high-energy tremors.

In the direct floor of coal seam no. 504, there are mostly shales. The floor of coal seam no. 504 is weak and able to heave.

The selected longwall began its run from near the downthrow side of fault with throw of 50 m. Activation of this fault by longwall mining at a close distance was probable. Local faults with throws of 0.6-4 m were present at the longwall field, which might have affected local stress concentrations.

The next longwall was running along the goaf made in the upper stage. The main gate was situated parallel to the field of the previous longwall, separated from the abandoned workings with five meters wide rib of coal or, additionally, by the gallery filled with filling.

Two coal seams nos. 418 and 502. deposited approximately 128 m and 69 m above coal seam no. 504 had been extracted in this area earlier. It influenced partially the relaxation of rock mass in this part of the mining field and was an advantageous factor influencing the stress level. Mining with selected longwall had been designed mostly under the goaf in coal seams nos. 418 and 502. At the end of its run, the selected longwall was driving under mining edges in the coal seams mentioned above, quasi parallel to the longwall face. These mining remnants affected the stress level in the rock mass, which was correlated with the observed high seismic activity.

High seismic activity was registered by the seismic network during mining of coal seam no. 504 with selected longwall under influence of mining edges in coal seams nos. 418 and 502 and where the destress exploitation of coal

seam no. 418 and 502 had not been performed. In this period there were 2200 events, with total released tremor energy of $1.2 \cdot 10^7$ J, including 11 high-energy tremors: 10 events with energy of 10^5 J ($1.68 \leq M_L < 2.21$) and 1 event with energy $2.0 \cdot 10^6$ J ($M_L = 2.37$). Presented values of the local magnitude in brackets have been calculated according to formula given by [14]. In the area of the selected longwall, there were 3014 events registered in a total, with total released tremor energy of $1.6 \cdot 10^7$ J. When the longwall face was under the abandoned workings in coal seams nos. 418 and 502, only two high-energy tremors with energy of 10^5 J occurred.

The factors mentioned above and the registered seismic activity determined the range of the applied active rockburst prevention.

3. Active rockburst prevention

Active rockburst prevention was based mainly on destress blasts in the roof rocks. These blasting stages were performed from longwall cross-cut, main gate, tail gate and, of course, longwall face, usually provoking immediate tremors, but in some cases also aftershocks. The inclinations of blastholes were determined with the use of the protractor and the diameter of each blasthole was 76 mm. The range of active rockburst prevention for the selected longwall and location of the epicenters of provoked tremors are shown in Fig. 1. Monthly longwall face advances are shown in Fig. 1. as well (grey broken lines).

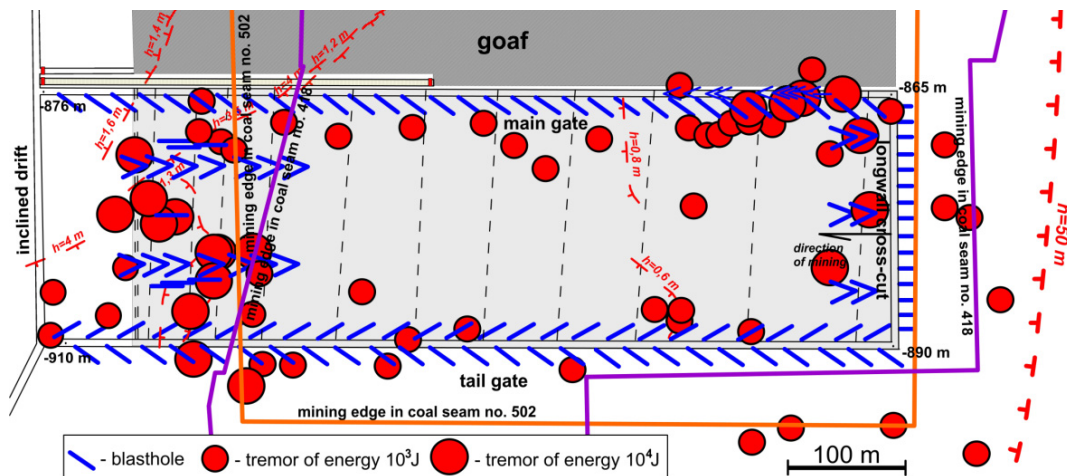


Fig. 1. Location of blastholes for destress blasts stages in roof rocks and provoked tremors.

Destress blasting stages were first performed from the longwall cross-cut. Blastholes were drilled to the east, to the direction of mining edges in coal seams nos. 418 and 502 and fault with throw 50 m. The aim of these blastings was to create a fracture zone in which the dissipation of strong tremors energy would take place and to provoke the first formation of the goaf. Blastholes were 15 m long and were drilled perpendicularly to the longwall cross-cut. The distance between blastholes was ca. 15 m. These blastholes were inclined upwards at the angle of 60° to the horizon. For each blasting stage, there were 2 to 6 blastholes drilled. 21 kg of explosive material (Emulinit PM) was loaded to each blasthole. 4 blastings stages (with the use of 15 blastholes) were performed in total. Tremors of energy between $1 \cdot 10^3$ J to $7 \cdot 10^3$ J were provoked.

When the longwall mining was in the start-up phase, two blasting stages from longwall face were performed, after 15 and 30 meters of longwall face advance. These blasting stages were performed to reduce stress concentrations in roof rocks ahead of the longwall face, and to make first goaf formation behind longwall face easier. During these two destress blasting stages, six blastholes with the length of 30 m (arranged in pairs: one pair in the middle of the longwall face, and the other pairs placed 40 m from main and tail gates) were performed every time. These blasthole orientations deviated from the longwall face to the north-west and south-west at an angle of ca. 70° , and were inclined upwards at the angle of 35° to the horizon. 48 kg of explosives were loaded into each

blasthole. Explosive material occupied ca. 10 m of each blasthole. The rest of each blasthole was filled with stemming. In total, 288 kg of Emulinit PM was detonated during each blasting. In both cases, these distress blasts provoked immediate tremors with the seismic energy of $5 \cdot 10^4$ J.

Distress blasts from the longwall face were restored and intensified in the area of mining edges in coal seams nos. 418 and 502. At that time, the total of 10 blasting stages were performed. During the first three blasting stages, 192 kg of explosives was detonated every time in 4 blastholes (48 kg per blasthole). Blastholes were arranged in pairs, drilled at a distance of ca. 70 m from the main and tail gate. In each pair, blastholes were deviated from longwall face to the north-west and south-west at an angle of ca. 70° . The length of each blasthole was 30 m. Blastholes were inclined upwards at the angle of 35° to the horizon. These blastings provoked tremors of energy $3 \cdot 10^4$ J, $5 \cdot 10^4$ J and $3 \cdot 10^4$ J, adequately. The average longwall advance between these blasting stages was ca. 21 m.

Because of the said high seismic activity and the correlated high level of rockburst hazard near mining edges in coal seam no. 418 and 502, the distress blasting stages were subsequently performed with increased amounts of blasted explosives. During four distress blasting stages from longwall face, 384 kg of explosives in four blastholes were detonated every time (96 kg per blasthole). During these blasting stages explosive material occupied nearly 20 m of blasthole and the rest was filled with stemming (Fig. 2). Blastholes were still arranged in pairs, located about 70 m from main and tail gate. Deviation of blastholes from longwall face remained the same. The length of blastholes had been increased to 50 m. Blastholes inclination was increased to 50° in relation to the horizon, which was determined optimally to both geological conditions and technical capability. The explosive material occupied almost 20 m of each blasthole length and was located in the layer of sandstones (Fig. 2). These distress blasting stages provoked immediate tremors of energy of $3 \cdot 10^4$ J, $4 \cdot 10^4$ J, $3 \cdot 10^4$ J and $7 \cdot 10^4$ J, respectively. On average, the blasts were performed at 26-m intervals of longwall face advance.

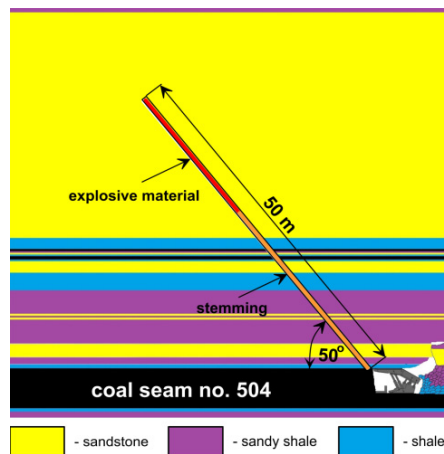


Fig. 2. Location of explosive material in roof rocks during blastings stages from longwall face.

Between the above-mentioned blasting stages with increased weight of explosives, additional blasting stages were performed to distress the rock mass ahead of longwall face in a wider range. During first two blasting stages, 192 kg of explosives were detonated in two blastholes (96 kg per blasthole) every time. The blastholes were drilled perpendicularly to the longwall face, at the distance of about 50 m from the main and tail gates and they were 50 m long. Blastholes inclination was 50° in relation to the horizon, so the explosive material was located in the layer of sandstones (Fig. 2). In the third additional blasting stage, one more blasthole in the middle of longwall face was drilled. Additional blasting stages adequately provoked immediate tremors of energy of $3 \cdot 10^4$ J, $2 \cdot 10^4$ J and $3 \cdot 10^4$ J.

Distress blasting stages were performed from main gate and tail gate as well. These blasting stages were performed to create a fracture zone where the dissipation of strong tremors energy would take place. Blastholes from main gate were drilled every 25 m. These blastholes were deviated from the main gate to the south-east at an angle of 30° . Blastholes from tail gate were drilled every 15 m, deviated alternating to the south-east and north-east at an angle of 30° . These blastholes were inclined upwards at the angle of 35° to the horizon. The length of these

blastholes was 30 m. 48 kg of explosives were loaded to each blasthole. During each blasting stage, 1 to 6 blastholes were drilled. In total, 13 blasting stages (with the use of 31 blastholes) were performed from the main gate, and 17 blasting stages (with the use of 52 blastholes) from the tail gate. Because of the diversified number of blastholes and the used weight of explosives, the energy of provoked tremors differed considerably. The tremors provoked by blastings from the main gate had the energy from $2 \cdot 10^3$ J to $9 \cdot 10^3$ J, and those from the tail gate - from $3 \cdot 10^3$ J to $1 \cdot 10^4$ J.

Some destress blasting stages were performed from the crossing of the longwall face with the main gate to prevent the hanging-up of roof rocks behind longwall face and to activate a process of goaf formation. Usually two blastholes in the direction of goaf were drilled, but in two cases there was only one blasthole. These blastholes had 15 m and were inclined upwards at the angle of 45° to the horizon. Blastholes were parallel to the main gate or were deviated from the main gate to the north-east and south-east at an angle of about 10° . In total, 11 blasting stages were performed in the described configuration. During 7 blasting stages, 48 kg per blasthole were detonated and during 4 blastings – only 36 kg per blasthole. During these blasting stages, 10 immediate tremors of energy between $2 \cdot 10^3$ J to $3 \cdot 10^4$ J were provoked. In one case tremor did not occur.

The effectiveness of applied active rockburst prevention was estimated via both the seismic effect method and analysis of seismic source parameters.

4. Seismic effect method

The effectiveness of destress blasts is connected with the stress release in rock mass and can be evaluated using seismic effect SE [1, 2]. Seismic effect SE is defined as the ratio of seismic energy released in the rock mass when blasting to the considered energy of the particular detonated charge [2] and can be calculated according to the following formula:

$$SE = \frac{E_{ICM}}{K_{ICM}Q} \quad [-] \quad (1)$$

where E_{ICM} is a seismic energy in [J] calculated by the seismic network in the investigated coal mine with the use of the numerical integration method, Q is a weight of the explosive charge in [kg] and K_{ICM} is a coefficient characterizing the conditions in the assigned mine [J/kg].

Coefficient K_{ICM} must be determined for the conditions in which the seismic monitoring is carried out and the seismic energy of registered seismic events is calculated in the same way [2]. Generally, this method uses the statistical data analysis of this seismic energy and the weight of the explosive charge from in situ monitoring. Coefficient K_{ICM} was determined for selected colliery as $K_{ICM} = 59.23$ J/kg [3].

The obtained value of the coefficient K_{ICM} was used to establish the classification system for the evaluation of SE . This classification was made according to the distribution of the data probability from calculated seismic effects according to equation (1). From the whole data set of seismic effect SE first quintile, median, third quintile and maximum were determined (1.4; 2.3; 3.5; 5.9, respectively). The outliers were determined as well. On the basis of the mentioned statistical parameters, the degrees of stress release due to destress blasting were distinguished. If the seismic effect SE was lower than first quintile, it meant that the effect of blasting was insignificant (registered energy released by blasting was less than 1.4 times the explosion energy). Seismic effect higher than maximum (outliers) was excellent (registered energy released by blasting was higher than 5.9 times the explosion energy). The classification system developed with which to evaluate SE values, based on criteria obtained from data distribution probabilities and according to equation (1), is presented in Table 1.

Although seismic energy is fundamental to the stress release effect and the SE calculations, it represents only a small proportion of the total blasting energy, with a considerable amount of the seismic energy observed in rock mass stress release. It should be noted that an evaluation of destress blasting effectiveness according to SE calculation alone represents an evaluation of only one main goal of destress blasting, that goal being stress release. The seismic effect of tremors provoked immediately was calculated.

Table 1. Classification system for the evaluation of SE in assigned colliery [3].

Seismic Effect (SE)	Evaluation of seismic effect	Percentage of data set
$SE < 1.4$	insignificant	20.7
$1.4 \leq SE < 2.3$	good	29.1
$2.3 \leq SE < 3.5$	very good	25.1
$3.5 \leq SE < 5.9$	extremely good	19.5
$SE \geq 5.9$	excellent	5.6

5. Seismic source parameters

Seismic source parameters characterize the focus of tremor. Seismic source parameters are calculated on the basis of records from seismic stations. The velocity and displacement spectra are considered. Based on these spectra, integrated in the frequency domain, the basic two independent seismic source parameters – the low-frequency spectral level Ω_o and the corner frequency f_o – can be determined [4, 5, 6]. With the use of these parameters the scalar seismic moment M_o can be calculated. It estimates the size of a tremor in the most reliable manner due to the assumed shear source mechanism. It can be calculated as follows [7]:

$$M_o = \frac{4\pi\rho V_c^3 R \Omega_o}{R_c F_c S_c} \text{ [Nm]} \quad (2)$$

where ρ is density in the source area, V_c is either the P or S-wave velocity in the source area (depending on the spectrum taken into consideration) and R is the distance between the source and the receiver. These three components in the denominator denote the correction for the radiation (R_c), free-surface (F_c) and site correction (S_c). The scalar seismic moment M_o allows for moment magnitude M_w calculation [8]:

$$M_w = \frac{2}{3} \log_{10} M_o - 6 \text{ [-]} \quad (3)$$

The seismic energy can be determined with the use of mean radiation coefficient $\langle R_c \rangle$ and J parameter (multiplied by 2 integration of square of velocity spectrum in the frequency domain), according to the formula presented by [9]:

$$E_o = 4\pi\rho V_c \langle R_c \rangle^2 \left(\frac{R}{F_c R_c} \right)^2 J \text{ [J]} \quad (4)$$

This parameter characterizes the dynamics of the processes occurring in the focus of the tremor. The seismic energy can be calculated separately from P and S-waves. The E_s/E_p ratio indicates the processes in the focal mechanism. In copper mines, the values of S to P wave energy ratio higher than 20 indicate that the DC (Double-Couple) forces are dominant in the focal mechanism [10]. The value of the ratio lower than 20 indicates that there are also other components of the mechanism solution present [10].

The source radius r_o is calculated based on the S-wave velocity V_s and the corner frequency f_o , applying the following formula [6]:

$$r_o = \frac{cV_s}{2\pi f_o} \text{ [m]} \quad (5)$$

The value of constant c depends on the applied source model [11, 12]. In Madariaga's source model adopted for calculations, constant c is 2.01 for the P-wave and 1.32 for the S-wave [6, 12]. Based on the calculated source radius r_o , the stress drop $\Delta\sigma$ can be determined using the following formula [6]:

$$\Delta\sigma = \frac{7}{16} \frac{M_o}{r_o^3} [\text{Pa}] \quad (6)$$

This parameter informs about the difference between the stress level before and after tremor occurrence and, therefore, can be the measure of stress release. It strongly depends on the source radius related to the adopted source model. The last source parameter is apparent stress σ_a corresponding to radiated energy per unit area and per unit slip. This parameter does not reflect the real stress drop. It can be calculated using the following formula [6]:

$$\sigma_a = \rho V_s^2 \frac{E}{M_o} [\text{J/m}^3] \quad (7)$$

The seismic source parameters were calculated separately from each seismogram, according to the formulas in the FOCI software shown above [13]. These parameters were then averaged for each tremors provoked by blasting. Only immediate tremors were taken into consideration.

6. Results

The seismic effects and seismic source parameters of destress blasting from longwall cross-cut (performed before the selected longwall began its run) are shown in Table 2.

Table 2. Seismic effects and seismic source parameters of destress blasting stages performed from longwall cross-cut.

No.	E_{ICM} [J]	Q [kg]	Seismic Effect (SE)	Ω_o	f_o [Hz]	M_o [Nm]	M_w	r_o [m]	E_o [J]	E_s/E_p	$\Delta\sigma$ [Pa]	σ_a [J/m ³]
1.	7.0E+03	126	0,9	7.39E-09	38.17	2.22E+10	0,67	27.1	2.90E+04	0,6	1.89E+06	4.44E+04
2.	3.0E+03	84	0,6	7.28E-09	35.81	1.55E+10	0,61	25.8	1.41E+04	0,5	1.09E+06	2.60E+04
3.	1.0E+03	42	0,4	5.39E-09	29.38	9.95E+09	0,51	29.7	3.72E+03	0,7	4.84E+05	1.33E+04

The energy E_{ICM} of provoked tremors is rather low, comparing with the amount of used explosives. In the light of the seismic effect method, these blastings are insignificant ($SE < 1.4$). Blasting stages from longwall cross-cut created a fracture zone and facilitated first goaf formation. However, configuration of blasting stages (used amount of explosives, number and length of blastholes) was not enough to provoke any additional processes in the rock mass.

The seismic source parameters of these tremors are characterized as follows: the low-frequency spectral level Ω_o is of the order of 10^{-9} (from $5.39 \cdot 10^{-9}$ to $7.39 \cdot 10^{-9}$, mean $6.69 \cdot 10^{-9}$), the corner frequency f_o is close to or higher than 30 Hz (from 29.38 to 38.17 Hz, mean 34.45 Hz), the source radius r_o (according to Madariaga's source model) is above twenty meters, but does not exceed 30 m (from 25.8 to 29.7 m, mean 27.53 m), the energy E_o calculated according to formula (4) is of the order of 10^3 - 10^4 J (from $3.72 \cdot 10^3$ J to $2.90 \cdot 10^4$ J, mean $1.56 \cdot 10^4$ J), the scalar seismic moment M_o is of order of 10^9 - 10^{10} Nm (from $9.95 \cdot 10^9$ to $2.22 \cdot 10^{10}$ Nm, mean $1.59 \cdot 10^{10}$ Nm) and the moment magnitude M_w varies from 0.51 to 0.67 (mean 0.6). Domination of non-shear mechanism is confirmed by the values of the ratio E_s/E_p (for every blasting stages lower than 1). The stress drop $\Delta\sigma$ in the focus, after blasting is of order of 10^5 - 10^6 Pa (from $4.84 \cdot 10^5$ to $1.89 \cdot 10^6$ Pa, mean $1.15 \cdot 10^6$ Pa), and the apparent stress σ_a is of 10^4 J/m³ (from $1.33 \cdot 10^4$ to $4.44 \cdot 10^4$ J/m³, mean $2.79 \cdot 10^4$ J/m³). For destress blasting stages from longwall cross-cut a clear dependence between values of seismic source parameters and amount of used explosives can be seen. In focus of provoked from longwall cross-cut tremors only explosion due to the detonation of explosives occurred. The values of seismic source parameters of these tremors will be then used as a reference point.

The seismic effects and seismic source parameters of destress blasting stages, performed from longwall face, are shown in Table 3. The energy E_{ICM} of provoked tremors is higher than in case of the blasting stages from longwall cross-cut, but the weight of used explosives was also higher.

Table 3. Seismic effects and seismic source parameters of destress blasting stages performed from longwall face.

No.	E_{ICM} [J]	Q [kg]	Seismic Effect (SE)	Ω_o	f_o [Hz]	M_o [Nm]	M_w	r_o [m]	E_o [J]	E_s/E_p	$\Delta\sigma$ [Pa]	σ_a [J/m ³]
1.	5.0E+04	288	2.9	5.82E-08	19.84	2.27E+11	1.2	49.7	1.28E+05	1.4	1.68E+06	2.46E+04
2.	5.0E+04	288	2.9	4.54E-08	17.4	1.56E+11	1.2	46.7	7.63E+04	1.7	8.61E+05	1.70E+04
3.	3.0E+04	192	2.6	1.78E-08	24.45	4.37E+10	0.93	30.8	7.44E+04	0.6	1.63E+06	3.53E+04
4.	5.0E+04	192	4.4	3.32E-08	18.06	1.25E+11	1.21	41.7	1.33E+05	1.3	1.04E+06	9.60E+03
5.	3.0E+04	192	2.6	4.32E-08	24.75	9.84E+10	0.99	34.3	1.22E+05	0.6	1.53E+06	4.50E+04
6.	3.0E+04	384	1.3	7.39E-08	19.31	2.65E+11	1.16	50.2	9.58E+04	0.6	1.06E+06	3.36E+04
7.	3.0E+04	192	2.6	1.27E-07	17.9	3.00E+11	1.2	49.3	1.62E+05	0.8	8.19E+05	2.63E+04
8.	4.0E+04	384	1.8	1.16E-07	15.74	2.04E+11	1.27	55.5	1.40E+05	1.2	6.56E+05	2.20E+04
9.	2.0E+04	192	1.8	7.23E-08	16.81	1.76E+11	1.14	50.2	6.94E+04	0.7	5.45E+05	1.71E+04
10.	3.0E+04	384	1.3	7.37E-08	17.54	1.24E+11	1.22	49.2	7.42E+04	0.6	8.16E+05	2.30E+04
11.	3.0E+04	288	1.8	5.75E-08	18.97	9.26E+10	1.21	41.8	6.07E+04	0.6	9.72E+05	1.95E+04
12.	7.0E+04	384	3.1	1.47E-07	12.41	3.14E+11	1.48	65.8	1.77E+05	3.9	7.73E+05	1.01E+04

According to the seismic effect method, these destress blasting stages provoked mainly some additional processes, because of which the rock mass achieves a new advantageous energy equilibrium. Only the seismic effect of blasting stages nos. 6 and 10 was insignificant. In 6 cases the effect was very good (including the strongest provoked tremor no. 12 within active rockburst prevention for the selected longwall). In 3 cases the effect was good. The seismic effect of blasting stage no. 4 was extremely good.

Seismic source parameters of tremors provoked by destress blasting stages from longwall face differ in many points from those provoked from the longwall cross-cut. The low-frequency spectral level Ω_o varies from $1.78 \cdot 10^{-8}$ to $1.47 \cdot 10^{-7}$ (mean $7.21 \cdot 10^{-8}$). The average low-frequency spectral level Ω_o of tremors provoked from the longwall face is ca. 90% higher than of tremors provoked from the longwall cross-cut. The corner frequency ranges from 12.41 to 24.75 Hz (mean 18.6 Hz). The average corner frequency f_o of tremors provoked from the longwall face is ca. 85% lower than of those provoked from the longwall cross-cut. The strongest provoked tremor has the lowest corner frequency f_o (12.41 Hz). The source radius r_o (according to Madariaga's source model) varies from 30.8 to 65.8 m (mean 47.1 m). The foci of tremors provoked from longwall face are larger. The average source radius r_o of these tremors is larger by ca. 40% in comparison to the average radius of tremors provoked from the longwall cross-cut. The strongest provoked tremor no. 12 was of the largest size (r_o equals 65.8 m). The energy E_o of tremors provoked from the longwall face is between $6.07 \cdot 10^4$ J and $1.77 \cdot 10^5$ J (mean $1.09 \cdot 10^5$ J), the scalar seismic moment M_o varies from $4.37 \cdot 10^{10}$ to $3.14 \cdot 10^{11}$ Nm (mean $1.77 \cdot 10^{11}$ Nm), and the moment magnitude M_w is in range from 0.93 to 1.48 (mean 1.19). Tremors provoked from the longwall face are stronger comparing with tremors provoked from the longwall cross-cut. The average energy E_o , average scalar seismic moment M_o and average moment magnitude M_w are, adequately, ca. 86%, 91% and 50% higher than the average of these parameters calculated for tremors provoked by the blasting stages from the longwall cross-cut. At large, it is an effect of the used weight of explosives, but concerning especially the strongest tremor no. 12 (the ratio E_s/E_p equals 3.9), additional slip mechanism in rock mass had been initiated. Of course, non-shear mechanism still dominates. Only the values of two parameters: the stress drop $\Delta\sigma$ and the apparent stress σ_a , are comparable with those calculated for the tremors provoked by the blasting stages from the cross-cut. The stress drop $\Delta\sigma$ in the focus after blasting is of 10^5 - 10^6 Pa (from $5.45 \cdot 10^5$ to $1.68 \cdot 10^6$ Pa, mean $1.03 \cdot 10^6$ Pa), and the apparent stress σ_a , excluding one case (tremor no. 4), is of 10^4 J/m³ (from $9.6 \cdot 10^3$ to $4.5 \cdot 10^4$ J/m³, mean $2.36 \cdot 10^4$ J/m³). As a result of blasting stages from the longwall face, the stress drop $\Delta\sigma$ occurred in larger areas comparing with blasting stages from the longwall cross-cut.

Tables 4 and 5 show the seismic effects and seismic source parameters of destress blasting stages adequately from main gate and tail gate. These blasting stages were performed at least 100 m ahead of the longwall face.

Generally, the seismic effect classifies destress blasting stages from main gate and tail gate as insignificant. Only one blasting stage from the tail gate (Table 5. tremor no. 13) is classified as very good. In general, despite the high weight of used explosives (in some cases comparable with blasting stages from the longwall face), blasting stages from the main gate and tail gate do not initiate any additional processes in the rock mass. These blasting stages created only a fracture zone due to detonation of the explosives.

Table 4. Seismic effects and seismic source parameters of destress blasting stages performed from main gate.

No.	E_{ICM} [J]	Q [kg]	Seismic Effect (SE)	Ω_o	f_o [Hz]	M_o [Nm]	M_w	r_o [m]	E_o [J]	E_s/E_p	$\Delta\sigma$ [Pa]	σ_a [J/m ³]
1.	6.0E+03	288	0,4	1.10E-08	28.23	1.83E+10	0,73	29.8	1.62E+04	0,7	9.30E+05	2.12E+04
2.	3.0E+03	96	0,5	1.73E-08	29.84	1.57E+10	0,65	28.1	1.39E+04	0,4	8.75E+05	2.55E+04
3.	2.0E+03	96	0,4	3.40E-09	31.58	9.40E+09	0,53	26.3	4.76E+03	0,7	6.65E+05	1.29E+04
4.	4.0E+03	96	0,7	7.82E-09	26.73	2.11E+10	0,79	32.4	1.13E+04	0,5	8.14E+05	1.31E+04
5.	3.0E+03	96	0,5	5.82E-09	27.33	1.31E+10	0,62	33.4	7.59E+03	0,3	5.67E+05	1.48E+04
6.	2.0E+03	48	0,7	4.25E-09	34.31	7.57E+09	0,45	20,1	4.98E+03	0,5	5.32E+05	8.22E+03
7.	7.0E+03	96	1,2	1.26E-08	26.46	1.94E+10	0,8	27.7	1.54E+04	0,3	7.06E+05	1.06E+04
8.	6.0E+03	96	1,1	1.81E-08	23.62	1.99E+10	0,81	28.1	2.45E+04	0,2	6.08E+05	1.65E+04
9.	2.0E+03	48	0,7	7.99E-09	27.64	7.83E+09	0,51	25.8	6.29E+03	0,2	4.75E+05	1.27E+04
10.	6.0E+03	96	1,1	1.54E-08	25.02	1.93E+10	0,77	29.1	3.17E+04	0,2	8.09E+05	1.96E+04
11.	4.0E+03	96	0,7	1.72E-08	23.49	1.99E+10	0,76	32.5	2.29E+04	0,2	7.84E+05	2.73E+04
12.	9.0E+03	192	0,8	2.22E-08	22.34	2.29E+10	0,84	26.2	6.57E+04	0,2	8.16E+05	3.11E+04
13.	6.0E+03	144	0,7	1.28E-08	23.49	2.27E+10	0,74	26.8	4.42E+04	0,2	8.79E+05	2.50E+04

Table 5. Seismic effects and seismic source parameters of destress blasting stages performed from tail gate.

No.	E_{ICM} [J]	Q [kg]	Seismic Effect (SE)	Ω_o	f_o [Hz]	M_o [Nm]	M_w	r_o [m]	E_o [J]	E_s/E_p	$\Delta\sigma$ [Pa]	σ_a [J/m ³]
1.	4.0E+03	240	0,3	2.14E-08	24.99	4.05E+10	0,78	35.2	2.39E+04	0,2	7.98E+05	2.22E+04
2.	3.0E+03	144	0,4	1.38E-08	28.79	1.50E+10	0,62	35	1.16E+04	0,2	8.03E+05	2.37E+04
3.	7.0E+03	96	1,2	1.13E-08	32.39	2.41E+10	0,79	25.6	3.49E+04	0,4	1.54E+06	3.09E+04
4.	7.0E+03	192	0,6	6.87E-08	28.03	4.51E+10	0,86	33.9	5.47E+04	0,1	1.50E+06	3.64E+04
5.	4.0E+03	192	0,4	2.52E-08	24.43	2.57E+10	0,78	37.7	2.12E+04	0,3	9.39E+05	2.34E+04
6.	3.0E+03	96	0,5	4.40E-09	31.61	1.33E+10	0,61	28.8	5.95E+03	0,3	8.54E+05	1.11E+04
7.	9.0E+03	192	0,8	1.16E-08	24	2.07E+10	0,82	33	2.09E+04	0,3	8.49E+05	1.95E+04
8.	7.0E+03	144	0,8	1.64E-08	25.6	2.37E+10	0,84	33	3.63E+04	0,2	1.09E+06	2.51E+04
9.	4.0E+03	96	0,7	1.56E-08	24.81	4.10E+10	0,74	32.2	2.19E+04	0,1	6.33E+05	1.58E+04
10.	4.0E+03	96	0,7	1.80E-08	28.99	5.33E+10	0,74	32.3	2.39E+04	0,3	9.44E+05	1.99E+04
11.	5.0E+03	144	0,6	2.17E-08	25.59	6.20E+10	0,8	32.5	4.07E+04	0,2	1.00E+06	2.10E+04
12.	9.0E+03	144	1,1	9.72E-09	30,09	1.83E+10	0,72	29	3.55E+04	0,1	1.41E+06	4.00E+04
13.	8.0E+03	48	2,8	1.00E-08	27.08	1.33E+10	0,62	29.9	1.63E+04	0,3	6.34E+05	1.64E+04
14.	1.0E+04	240	0,7	1.93E-08	23.15	4.44E+10	0,93	38	4.80E+04	0,2	1.14E+06	3.14E+04
15.	1.0E+04	192	0,9	1.97E-08	23.91	3.61E+10	0,89	36.7	4.84E+04	0,7	1.26E+06	3.85E+04
16.	6.0E+03	144	0,7	2.04E-08	22.79	2.67E+10	0,85	31.5	4.72E+04	0,4	1.07E+06	2.97E+04
17.	4.0E+03	96	0,7	1.20E-08	27.32	1.57E+10	0,68	34.4	1.94E+04	0,7	1.11E+06	3.09E+04

The values of the seismic source parameters of tremors provoked by blasting stages from main and tail gates do not differ much from each other. In case of destress blasting stages from the main gate: the low-frequency spectral level Ω_o is of 10^{-8} - 10^{-9} (from $3.4 \cdot 10^{-9}$ to $2.22 \cdot 10^{-8}$, mean $1.2 \cdot 10^{-8}$), the corner frequency f_o is between 22.34 and 34.31 Hz (mean 26.93 Hz), the source radius r_o varies from 20.1 to 33.4 m (mean 28.18 m), the energy E_o is of 10^3 - 10^4 J (from $4.76 \cdot 10^3$ J to $6.57 \cdot 10^4$ J, mean $2.07 \cdot 10^4$ J), the scalar seismic moment M_o is of 10^9 - 10^{10} Nm (from $7.57 \cdot 10^9$ to $2.29 \cdot 10^{10}$ Nm, mean $1.67 \cdot 10^{10}$ Nm), the moment magnitude M_w varies from 0.45 to 0.84 (mean 0.69), the ratio E_s/E_p achieves maximum 0.7 (mean 0.36) – which indicates a non-share mechanism, the stress drop $\Delta\sigma$ in the focus after blasting is of 10^5 Pa (from $4.75 \cdot 10^5$ to $9.3 \cdot 10^5$ Pa, mean $7.28 \cdot 10^5$ Pa), and the apparent stress σ_a is of 10^3 - 10^4 J/m³ (from $8.22 \cdot 10^3$ to $3.11 \cdot 10^4$ J/m³, mean $1.83 \cdot 10^4$ J/m³). In case of destress blasting stages from the tail gate: the low-frequency spectral level Ω_o is of 10^{-8} - 10^{-9} (from $4.4 \cdot 10^{-9}$ to $6.87 \cdot 10^{-8}$, mean $1.88 \cdot 10^{-8}$), the corner frequency f_o varies from 22.79 to 32.39 Hz (mean 26.68 Hz), the source radius r_o is between 25.6 to 38 m (mean 32.86 m), the energy E_o is of 10^3 - 10^4 J (from $5.95 \cdot 10^3$ J to $5.47 \cdot 10^4$ J, mean $3 \cdot 10^4$ J), the scalar seismic moment M_o is of order of 10^{10} Nm (from $1.33 \cdot 10^{10}$ to $6.2 \cdot 10^{10}$ Nm, mean $3.05 \cdot 10^{10}$ Nm), the moment magnitude M_w is between 0.61 and 0.93 (mean 0.77), the ratio E_s/E_p achieves maximum 0.7 (mean 0.3) – which indicates a non-share mechanism, the stress drop $\Delta\sigma$ in the focus after blasting is of 10^5 - 10^6 Pa (from $6.33 \cdot 10^5$ to $1.54 \cdot 10^6$ Pa, mean $1.03 \cdot 10^6$ Pa), and the apparent stress σ_a is of 10^4 J/m³ (from $1.11 \cdot 10^4$ to $4 \cdot 10^4$ J/m³, mean $2.56 \cdot 10^4$ J/m³). During blasting stages from the tail gate, there were usually more explosives detonated in comparison to the blasting stages from the main gate.

When other parameters of the blasting stages and geological and mining conditions were similar, only the amount of detonated explosives affected the values of seismic source parameters. For example, the average energy E_o is higher by ca. 45%, average scalar seismic moment M_o is higher by ca. 83% and average moment magnitude M_w is higher by ca. 11% in comparison to these parameters of tremors provoked by the destress blasting stages from the main gate.

Another destress blasting stages to goaf formation were performed from the main gate. The seismic effects and seismic source parameters of these blasting stages are shown in Table 6. In these blasting stages, there was usually a low amount of explosives used (from 48 to 96 kg). The explosive material occupied about 7 m of each blasthole. However, the location of blastholes during these blasting stages was of significance.

Table 6. Seismic effects and seismic source parameters of blasting stages to goaf formation.

No.	E_{ICM} [J]	Q [kg]	Seismic Effect (SE)	Ω_o	f_o [Hz]	M_o [Nm]	M_w	r_o [m]	E_o [J]	E_s/E_p	$\Delta\sigma$ [Pa]	σ_a [J/m ³]
1.	2.0E+03	48	0,7	1.53E-08	23.41	1.59E+10	0,69	35.4	7.42E+03	0,1	3.67E+05	9.14E+03
2.	2.0E+04	96	3.5	6.07E-08	16.33	6.71E+10	1.17	42.5	8.16E+04	0,2	6.78E+05	1.61E+04
3.	2.0E+03	48	0,7	9.24E-09	24.63	1.44E+10	0,67	30,2	9.67E+03	0,1	4.65E+05	1.39E+04
4.	2.0E+04	96	3.5	5.76E-08	18.59	7.11E+10	1.14	41.3	7.91E+04	0,2	8.66E+05	2.06E+04
5.	2.0E+04	96	3.5	6.63E-08	21.35	6.94E+10	1.11	37.2	8.90E+04	0,3	1.19E+06	2.29E+04
6.	3.0E+04	96	5.3	4.93E-08	19.88	5.76E+10	1.08	38.7	7.88E+04	0,4	1.02E+06	2.92E+04
7.	9.0E+03	96	1.6	6.82E-08	17.49	7.89E+10	1.17	43.5	9.81E+04	0,1	8.69E+05	2.33E+04
8.	1.0E+04	72	2.3	1.35E-07	21.82	1.12E+11	1.05	48.7	4.81E+04	0,3	9.34E+05	2.06E+04
9.	9.0E+03	72	2.1	3.36E-08	21.41	3.69E+10	0,96	35.8	3.89E+04	0,2	7.55E+05	1.82E+04
10.	7.0E+03	72	1.6	3.97E-08	23.52	3.21E+10	0,89	32.9	2.80E+04	0,2	7.20E+05	1.53E+04

The energy E_{ICM} of provoked tremors is mostly higher than it would appear from the weight of used explosives. According to the seismic effect method, 80% of these blasting stages provoked additional processes in the rock mass, enabling achievement of a new advantageous energy equilibrium. Only in two cases (tremors nos. 1 and 3) the seismic effect is insignificant. In four cases the effect is extremely good, while in 3 cases it is good. In one blasting stage the effect is very good.

The seismic source parameters of tremors provoked by blasting stages from the crossing of the longwall face with main gate are as follows: the low-frequency spectral level Ω_o is of 10^{-7} - 10^{-9} (from $9.24 \cdot 10^{-9}$ to $1.35 \cdot 10^{-7}$, mean $5.35 \cdot 10^{-8}$), the corner frequency f_o is lower than 25 Hz (from 16.33 to 24.63 Hz, mean 20.84 Hz), the source radius r_o (according to Madariaga's source model) in all cases exceeds thirty meters (from 30.2 to 48.7 m, mean 38.62 m), the energy E_o is of 10^3 - 10^4 J (from $7.42 \cdot 10^3$ J to $9.81 \cdot 10^4$ J, mean $5.59 \cdot 10^4$ J), the scalar seismic moment M_o is of 10^{10} - 10^{11} Nm (from $1.44 \cdot 10^{10}$ to $1.12 \cdot 10^{11}$ Nm, mean $5.55 \cdot 10^{10}$ Nm), and the moment magnitude M_w varies from 0.67 to 1.17 (mean equals 1). Domination of the non-shear mechanism is confirmed by the values of the ratio E_s/E_p (lower than 0.5 for every blasting stage). In the foci of these tremors, there was probably an implosion. The stress drop $\Delta\sigma$ in the focus after blasting is of 10^5 - 10^6 Pa (from $3.67 \cdot 10^5$ to $1.19 \cdot 10^6$ Pa, mean $7.86 \cdot 10^5$ Pa), and the apparent stress σ_a is of 10^3 - 10^4 J/m³ (from $9.14 \cdot 10^3$ to $2.92 \cdot 10^4$ J/m³, mean $1.89 \cdot 10^4$ J/m³). In comparison to the seismic source parameters of tremors provoked by destress blasting stages from the longwall cross-cut, the average low-frequency spectral level Ω_o is higher by ca. 700%, the average corner frequency f_o is lower by ca. 40%, the average source radius r_o is larger by ca. 40%, the average energy E_o is higher by ca. 258%, the average scalar seismic moment M_o is higher by ca. 259%, and the average moment magnitude M_w is higher by ca. 66%. The stress drop $\Delta\sigma$ and the apparent stress σ_a are at comparable levels. However, the destress blasting stages to goaf formation covered larger areas in comparison to the destress blasting stages performed from the longwall cross-cut.

7. Conclusions

Active rockburst prevention enables longwall mining under difficult geological and mining conditions. Destress blasts play a significant role in rockburst prevention. These blastings are usually performed from the longwall face and the main and tail gates, in various configurations. The main parameters of blasting stages include: number and length of blastholes, location of blastholes and their inclination to the horizon and, of course, weight of the explosives. Effectiveness of destress blasts is correlated with the destress range and with reaching of a new

advantageous energy equilibrium state by the rock mass due to the stress drop. Estimation of destress blasting effectiveness is particularly important for safe extraction of coal seams. Such a calculation has been performed for the assigned longwall in coal seam no. 504. in one of the hard coal mines in the Polish part of the USCB.

This effectiveness can be estimated with the use of seismic parameters. The energy of provoked tremors is used in the seismic effect method. This primary method has been adapted to the local conditions (geology, mining system, blasting parameters, seismic network parameters etc.) [3]. According to this method, destress blasting stages from the longwall face, and especially destress blasting stages for the goaf formation performed from the crossing of the longwall face with the main gate provided better effects in comparison to the used weight of explosives. On the example of destress blasting stages for goaf formation, it has been shown that proper location of blastholes can provide incommensurable effects, despite detonation of a low amount of explosives. Destress blasting stages performed from the longwall cross-cut, main gate and tail gate did not activate any other processes in the rock mass. The values of seismic effects correspond to the weight of the used explosives.

The seismic source parameters provide additional information about the foci of tremors and processes occurring in them. From this point of view, these parameters could be useful for the estimation of destress blasting effectiveness. These parameters have been calculated for tremors provoked by destress blasting stages within active rockburst prevention for the assigned longwall in coal seam no. 504. The differences between tremors provoked by destress blasting stages from the longwall face and crossing of longwall face with the main gate and the rest of the blasting stages in most cases can be seen clearly. These tremors are characterized mainly by lower corner frequency f_o , larger source radius r_o , higher energy E_o and higher moment magnitude M_w . On the basis of ratio E_s/E_p in the focus of the strongest tremor (provoked by the blasting from longwall face), some share of slip mechanism occurred. In the foci of tremors provoked by the blasting stages from the crossing of the longwall face with the main gate, domination of the non-shear mechanism has been confirmed. According to the geological and mining conditions in the foci of these tremors, implosion was probably predominant. The stress drop $\Delta\sigma$ and the apparent stress σ_a are comparable for all the analyzed tremors. However, in cases of blasting stages from the longwall face and the crossing of longwall face with the main gate, a larger area was destressed.

Acknowledgements

The project was supported by the Centre for Polar Studies, University of Silesia, Poland - The Leading National Research Centre (KNOW) in Earth Sciences 2014-2018 and Young Scientists Project No. 1M-0416-001-1-01.

References

- [1] S. Knotek, Z. Matusek, A. Skrabis, P. Janas, B. Zamarski, B. Stas, Research of geomechanics evaluation of rock mass due to geophysical method, VVUU, Ostrava, 1985, (in Czech).
- [2] P. Konicek, K. Soucek, L. Stas, R. Singh, Long-hole destress blasting for rockburst control during deep underground coal mining, International Journal of Rock Mechanics & Mining Sciences 61 (2013) 141–153.
- [3] Ł. Wojtecki, P. Konicek, Estimation of active rockburst prevention effectiveness during longwall mining under disadvantageous geological and mining conditions, Journal of Sustainable Mining 15(1) (2016) 1–7.
- [4] D.J. Andrews, Objective determination of source parameters and similarity of earthquakes of different size, in: S. Das, J. Boatwright, C.H. Scholtz, eds., Earthquake Source Mechanics, Vol. 6. Am. Geophys. Union, Washington, D.C., 1986, pp 259–267.
- [5] J.A. Snoke, Stable determination of (Brune) stress drops. Bull. Seism. Soc. Am. 64 (1987) 1295–1317.
- [6] A. Udías, R. Madariaga, E. Buforn, Source Mechanisms of Earthquakes: Theory and Practice, Cambridge University Press, 2014.
- [7] K. Aki, P.G. Richards, Quantitative Seismology. Theory and Methods, Freeman, San Francisco, 1984.
- [8] T.C. Hanks, H. Kanamori, A moment magnitude scale, J. Geophys. Res. 84 (1979) 2348–2350.
- [9] S.J. Gibowicz, A. Kijko, An Introduction to Mining Seismology, Academic Press, San Diego, 1994.
- [10] G. Lizurek, P. Wiejacz, Moment Tensor Solution and Physical Parameters of Selected Recent Seismic Events at Rudna Copper Mine, in: A.F. Idziak, R. Dubiel (eds.), Geophysics in Mining and Environmental Protection, Geoplanet: Earth and Planetary Sciences 2, 2011, pp 11.
- [11] J. N. Brune, Tectonic stress and the spectra of seismic shear waves from earthquakes, J. Geophys. Res. 75 (1979) 4997–5009.
- [12] R. Madariaga, Dynamics of an expanding circular fault. Bull. Seism. Soc. Am. 66 (1979) 639–666.
- [13] G. Kwiatek, P. Martínez-Garzón, M. Bohnhoff, HybridMT: A MATLAB/shell environment package for seismic moment tensor inversion and refinement, Seismol. Res. Lett., 2016.
- [14] J. Dubinski, Z. Wierchowska, Methods for the calculation of tremors seismic energy in the Upper Silesia. Katowice, Poland: Central Mining Institute, no. 591, 1973 (in Polish).